JOURNAL OF MATERIALS SCIENCE: MATERIALS IN MEDICINE 4 (1993) 76–82

Stoichiometry of hydroxyapatite: influence on the flexural strength

A. ROYER, J. C. VIGUIE
CEREM/DEM/LGM, CENG, 85X, 38041 Grenoble Cedex, France
M. HEUGHEBAERT, J. C. HEUGHEBAERT
Laboratoire de Physico-Chimie des Solides, 38 rue des 36 Ponts, 31400 Toulouse, France

This paper reports results on the sintering behaviour of hydroxyapatite (HAP) for various compositions and its resultant flexural strength. The HAP decomposition occurs at higher temperatures for sintered compacts than for powder and their OH stoichiometry depends on the porosity-closing temperature. The mechanical behaviour of HAP depends on its composition: the best results are obtained for HAP containing tricalcium phosphate (TCP), whereas for nearly pure HAP the flexural strength decreases to the lowest results corresponding to HAP containing CaO. It is suggested that the strengthening of HAP by TCP involves surface compression due to the $\beta \rightarrow \alpha$ TCP transformation.

1. Introduction

Hydroxyapatite [HAP; $Ca_{10}(PO_4)_6(OH)_2$] is the main mineral component of calcified tissues [1]. Since the work of Jarcho *et al.* [2, 3] on dense sintered synthetic HAP, this ceramic is known to be totally biocompatible and to form a direct bond with the neighbouring bone. However, the lack of mechanical strength in this bioceramic is a serious drawback. It can be used only for applications where no important stress has to be borne [4]. Two proposed solutions to this problem are to use the properties of HAP as a surface layer on titanium implants [5] or to elaborate a composite with better mechanical properties with HAP as the matrix [6, 7]. However, before considering an even more complex system as a composite, a thorough knowledge of the matrix is necessary. Many investigations concerning HAP have been published, but because the name HAP is used for a wide range of compositions beyond the formula given above, great caution must be exercised when comparing different results. The exact composition seems to be an important parameter, since the biodegradation rate, for example, depends on it [8]. When the atomic ratio Ca/P of the initial powder is different from 1.667, the ceramic, sintered at $T > 1000\,^{\circ}C$, is generally composed of several phases such as HAP + calcia (CaO), when Ca/P > 1.667 or HAP + tricalcium phosphate [$Ca_3(PO_4)_2$; TCP], when Ca/P < 1, 1667 [9]. This study was devoted to the influence of the composition on the sintering and to the resultant mechanical properties of HAP.

2. Experimental

2.1. Sample preparation

The HAP powder was prepared at the LPCS, Toulouse. HAP was precipitated in an aqueous medium by slow addition of diammonium phosphate [$(NH_4)_2(HPO_4)$] solution containing NH_4OH to a boiling calcium nitrate [$Ca(NO_3)_2$] solution also containing NH_4OH. After the addition, the suspension was refluxed before being filtered without washing. Different calcium stoichiometries were prepared by using more or less $Ca(NO_3)_2$ in the process. The exact Ca/P, TCP/HAP or CaO/HAP weight ratio was measured by X-ray diffraction (XRD) on a sample heated overnight at 900 °C. A "calibration" graph, relating the ratio of the surfaces of the principal peaks to the Ca/P ratio measured by chemical analysis, was used.

After filtration the slurry was spray-dried. The granulated powder was then fired at 800 °C for 5 h. The powder had a specific surface, S, of 18 $m^2 g^{-1}$ by the Brunauer–Emmett–Teller (BET) method for HAP Ca/P = 1.667. The S_{BET} decreased with the Ca/P ratio down to 5 $m^2 g^{-1}$ for TCP Ca/P = 1.5. The powder was composed of spheroidal granulates of 50–60 μm diameter. The samples were premoulded at 100 MPa in a uniaxial press of diameter 28 mm and then isostatically compacted at 400 MPa. The granulates were totally destroyed. The resultant green density, over 55% theoretical density M_{vth}, depends on the Ca/P ratio [10]. The samples were sintered in air for 5 h at 1250 °C (heating rate 100 °C h^{-1}, cooling rate 200 °C h^{-1}).

2.2. Sample testing

Thermogravimetric analyses were made on a Setaram TG 85 thermobalance and the dilatometric analyses on an Adamel DI 24 dilatometer. The density and the porosity of the sintered samples were measured by the Archimedes liquid-displacement method in ethanol. Microstructures were observed by scanning electron

0957–4530

microscopy (SEM) using a Jeol in the secondary-electron image (SEI) mode: the samples were first polished with diamond paste, then thermally etched and coated with a fine layer of gold. The average grain size was estimated from the SEM micrographs using the linear-intercept method. The different phases were located using back-scattered electron imaging (BEI) on polished samples covered with carbon. XRD patterns were recorded on a Philips goniometer on powdered samples using cobalt radiation. The lattice parameters were determined by the least-squares method using the HAP reflections 0 0 2, 1 1 2, 3 0 0, 2 0 2, 3 1 0, 2 2 2, 2 1 3, 3 2 1, 4 1 0 and 0 0 4. Quantitative measurements of the evolution of the β-TCP into α-TCP were given by the evolution of the ratio of the 0 3 4 α-TCP on the $0\,2\,\bar{1}0$ β-TCP peaks. The strength of HAP was assessed using flexural testing, since this technique is more sensitive and critical than compressive strength testing. The strength was measured on discs according to the American Society for Testing and Materials standard F394-78 biaxial flexure test corresponding to the piston-on-three-balls geometry. The samples were tested as received from sintering (diameter 22 mm and thickness 3.5 mm). An Instron testing unit was used with a crosshead speed of 100 μm min^{-1}.

3. Results and discussion

3.1. Sintering of HAP

3.1.1. Dilatometric analysis

The sintering of HAP starts around 900–1000 °C (Fig. 1). The final density of 98% theoretical (3.16 g cm^{-3}) is obtained for $T = 1250$ °C. The difference in the dilatometric sintering behaviour of materials with different Ca/P ratios is shown in Fig. 1: the presence of CaO blocks the densification of HAP, whereas TCP only delays the sintering process. The sintering of TCP is interrupted at 1180 °C by the allotropic transformation $\beta \rightarrow \alpha$ because of the increase of volume due to this transformation [11] and the density even decreases slightly. Up to 40% TCP the sample sinters as HAP does; for higher concentrations of TCP the behaviour resembles that of TCP.

3.1.2. Thermogravimetric analysis

A powder of HAP previously fired at 800 °C loses different types of water when reheated: reversibly adsorbed water below 200 °C to strongly bound water up to 800 °C [12], but no reaction occurs. Then the gradual OH condensation causes HAP to turn into an oxyhydroxyapatite $[Ca_{10}(PO_4)_6(OH)_{2-2x}O_x]$ [9, 13]. At higher temperatures the decomposition of this product into tetracalcium phosphate monoxide ($Ca_4P_2O_9$; TCPM) and α-TCP occurs. As long as HAP has not been decomposed, the OH dehydration reaction is reversible. The sintering of the compact to a dense ceramic modifies the dehydration process (Figs 2 and 3): first the dehydration of HAP stops around 1200 °C during the last stage of the sintering of HAP, as the open porosity disappears. The exchanges with the atmosphere are then restricted to the surface. This is true for the dehydration as well as for the rehydration. The decomposition takes place 100 °C higher because the HAP structure is stabilized by the maintained OH groups (Fig. 3).

Fig. 4 shows the weight loss of the same samples as those in the dilatometric study (Fig. 1). They all lose variable quantities of readsorbed water up to 800 °C, the calcination temperature. For HAP + CaO a slight weight loss occurs at 600 °C, which is due to the dehydration of $Ca(OH)_2$ into CaO. The TCP loses all of its water between 800 and 1000 °C. It is the end of the transformation of the apatitic TCP $[Ca_9(HPO_4)(PO_4)_5(OH)]$ into β-TCP [14] which also occurs in the samples HAP + TCP. The ending of the loss of water due to the HAP and TCP transformations occurs at different temperatures for the different samples, containing mainly HAP. These temperatures correspond to the end of their sintering when the open porosity closes, as can be seen in Fig. 1.

The fact that the OH stoichiometry depends on the porosity-closing temperature is confirmed by the evolution of the lattice parameter a of HAP: for temperatures below 1150 °C, before the open porosity disappears, $a = 0.9428$ nm, which is the value for an OH stoichiometric HAP [15]; the OH lost are regained during cooling. For $T > 1150$ °C a contraction

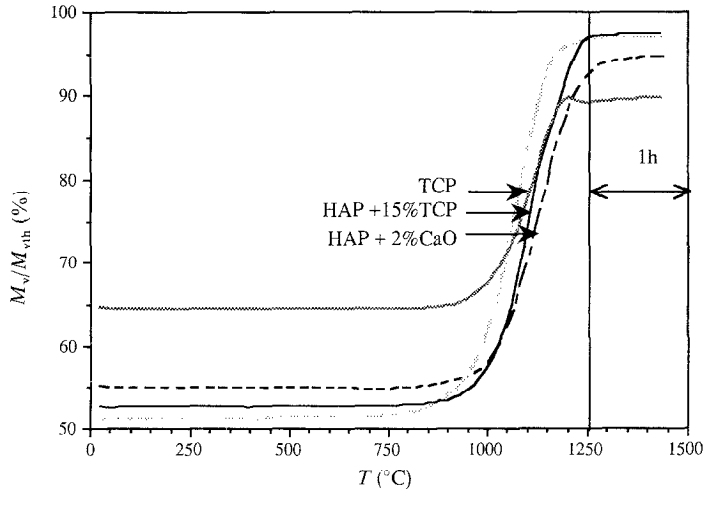

Figure 1 Densification curves for various calcium stoichiometries.

of a indicates the permanent loss of some OH groups [9, 13] (Fig. 5), but a does not decrease for higher temperatures. The OH groups are lost until the porosity is closed, then there can be no further loss for higher temperatures or gain during the cooling. The bulk of the sintered product is then made of oxyhydroxyapatite.

3.2. Morphology of HAP sintered samples

The correlation between two SEM images of the same sintered sample, BEI for the composition and SEI for the microstructure, allows the identification of the different phases. For the sample containing 11 wt % TCP (cf. Fig. 6), the darker zone in the BEI image corresponds to the TCP, which is less dense than the HAP matrix. The same zone, after revealing the microstructure, appears to have a different structure from the HAP matrix: the grains are much smaller than the surrounding matrix grains. For samples containing an excess of calcium, very small, white, intense and dispersed spots may represent CaO but no second microstructure is visible. Energy-dispersive X-ray (EDX) analysis and electron-microprobe analysis confirmed the identification of TCP with a lower calcium concentration in the dark area and of CaO with a higher one in the white spots referring to the HAP matrix.

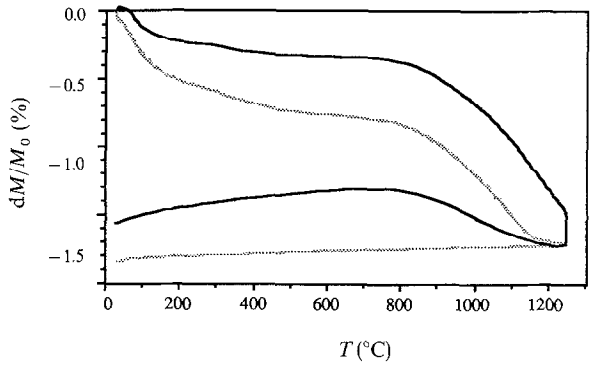

Figure 2 Weight loss of HAP when heated up to 1250 °C: (——) as powder and (. . . . .) as compact.

Another aspect of the composition on the microstructure is the increase in the grain size of HAP as Ca/P decreases (Fig. 7). The samples containing CaO have smaller grains and a more regular size distribution, whereas samples containing TCP seem to suffer from abnormal grain growth. CaO in HAP acts as a pinning agent of the grain boundary, like a non-mobile second phase which limits the grain growth and the densification [16]. The TCP, conversely, is a mobile phase with a tendency to agglomerate as the temperature increases (Fig. 8). Because of this migration and coalescence, a layer of TCP is formed at the surface. Its thickness increases with temperature and time (Fig. 9). The XRD analysis of the surface showed that the TCP is mainly α-TCP.

3.3. Strength of the sintered HAP samples

3.3.1. Pure HAP

The effect of sintering temperature on the grain size, d, the specific gravity, M_v, and the biaxial flexure strength, σ_f, is shown in Fig. 10. A classical sintering feature appears: d does not increase until M_v is almost maximum at the end of the densification [17]. The strength increases as the porosity, p, disappears, as is commonly observed for ceramics [18]

$$\sigma_f = \sigma_{f0}\exp(-bp)$$

where for HAP $\sigma_{f0} = 113$ MPa and $b = 0.06$. Once the open porosity has disappeared, σ_f is at a maximum. It decreases for higher temperatures as d increases. At first, for small grain sizes in dense samples, σ_f is constant: the critical flaw of Griffiths theory is not related to the grain size but depends on the preparation process (Fig. 11) [19]. Then σ_f decreases according to the Petch–Hall law $\sigma_f = Kd^{-1/2}$. For larger grain sizes, the σ_f of the Petch–Hall law corresponds to a larger grain size than the average grain size. As HAP produces an exaggerated grain growth, the critical flaw is then related to the largest grain.

3.3.2. Samples with different Ca/P ratios

The term HAP covers a wide range of calcium stoichiometries: Ca/P = 1.62 for De With *et al.* [20] to

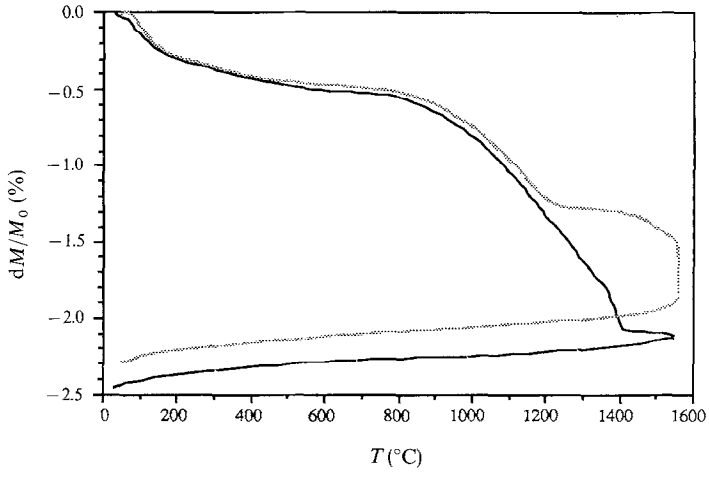

Figure 3 Weight loss of HAP when heated up to 1550 °C: (——) as powder and (. . . . .) as compact.

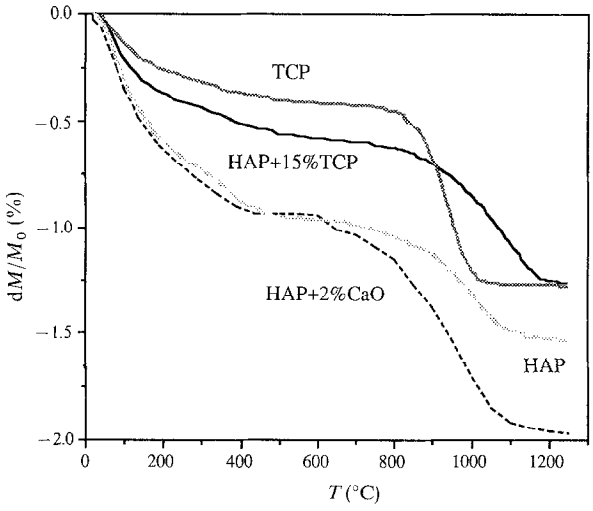

Figure 4 Weight loss for various calcium stoichiometries.

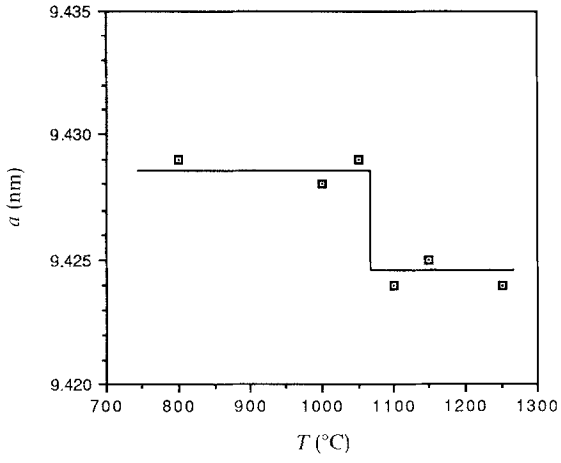

Figure 5 HAP cell parameter a versus the sintering temperature.

Ca/P = 1.69 for Akao *et al.* [21]. The mechanical behaviour of these HAPs depends on their composition. The evolution of the strength versus the composition of the samples is shown in Fig. 12 for two sintering temperatures, 1150 and 1250 °C. Four regions are visible. (1) When TCP is the major component, the results are poor because TCP does not sinter as well as HAP. (2) When HAP is the major component, σ_f is at a maximum of 150 MPa. (3) Around the stoichiometry of HAP, the results are widely dispersed. (4) The lowest σ_f are for HAP + CaO. It therefore appears that stoichiometry is not the best composition for mechanical strength. The wide range of results around the stoichiometry may be associated with the difficulties in obtaining and measuring this stoichiometry exactly. As the different phases, including CaO, have very similar dilatation coefficients [10], the weakening due to CaO cannot be attributed to thermally built-up constraints. However, the hydration of CaO is known to build up stress due to the greater volume of the resultant hydroxide. For dense samples the degradation is reported to occur at the surface [22]: the wedging action at the bottom of the surface cracks enlarges them and weakens the material.

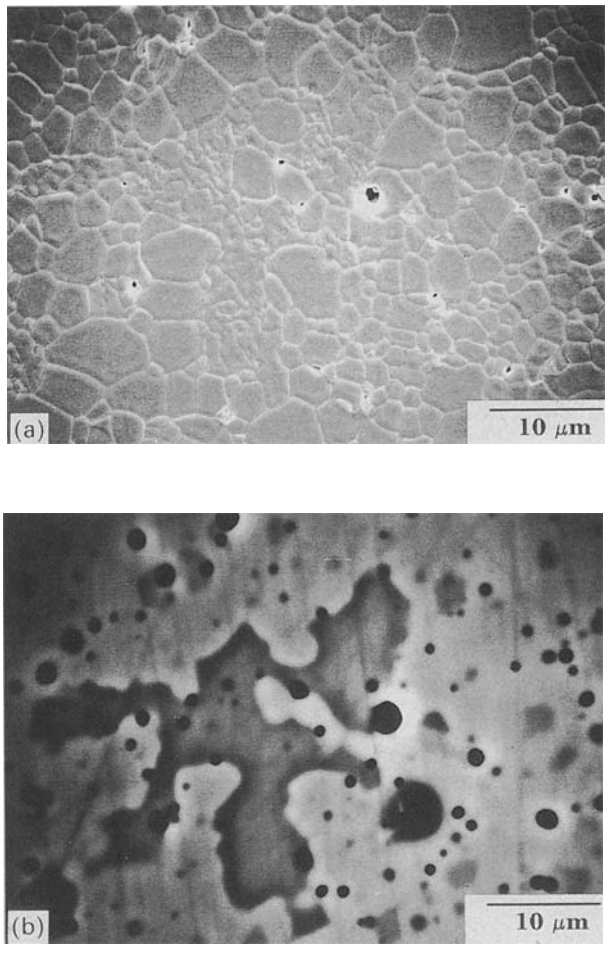

Figure 6 Correspondence between (a) the composition (BEI) and (b) the microstructure (SEI) of an HAP + TCP sample.

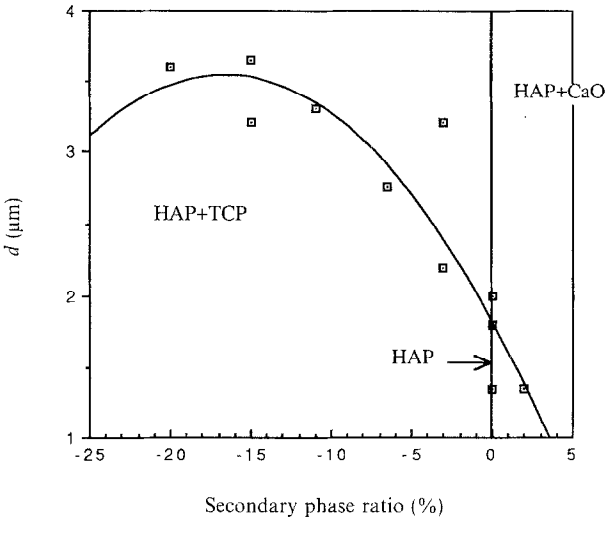

Figure 7 Influence of Ca/P on the average grain size of the HAP matrix.

3.3.3. β → α TCP phase transformation

TCP appears to play an active role in the strengthening of HAP. Fig. 13 shows the evolution of the strength with the sintering temperature for two samples of HAP + TCP. In the second sample,

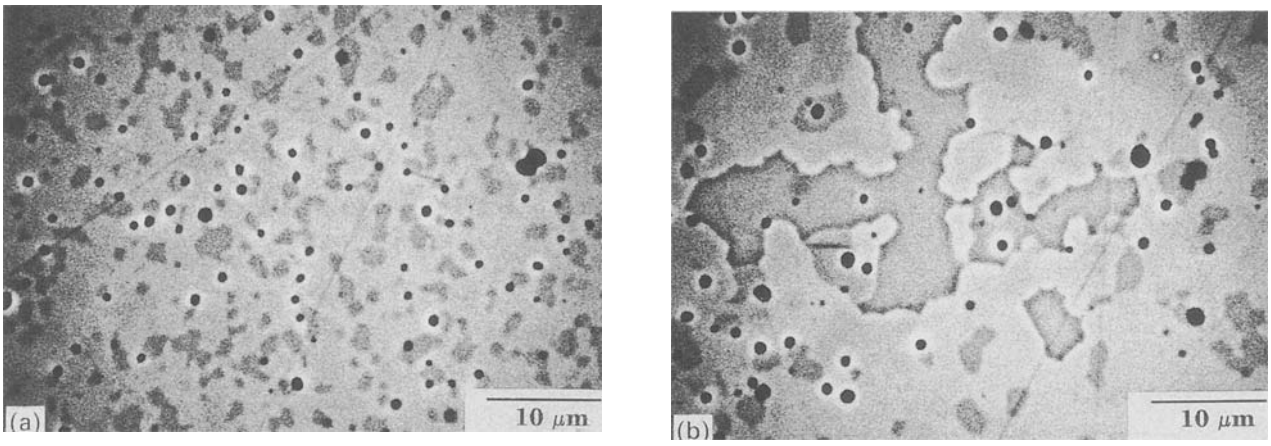

Figure 8 TCP agglomeration with temperature, 1200–1250 °C.

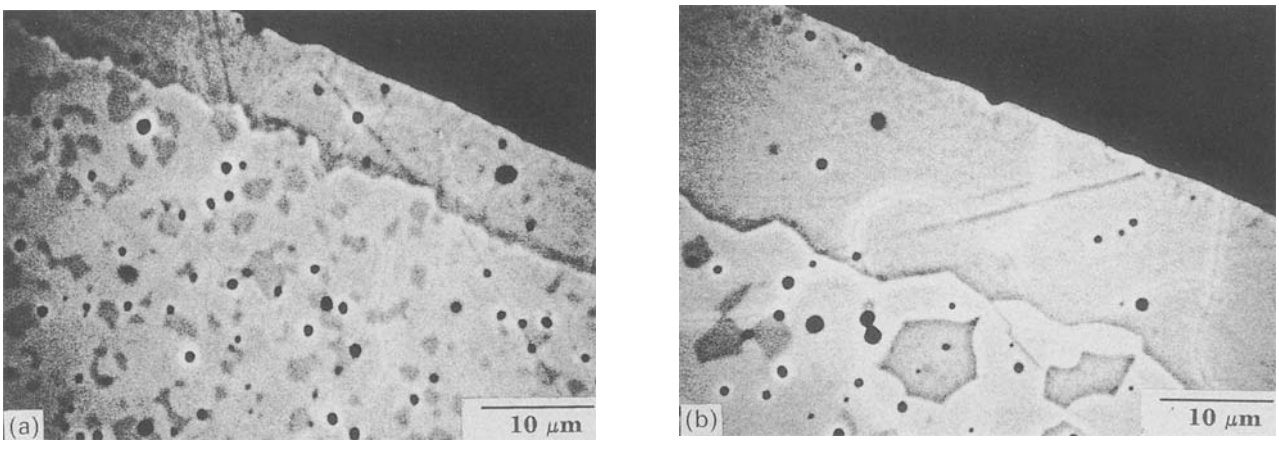

Figure 9 TCP layer on the surface, 1200–1300 °C.

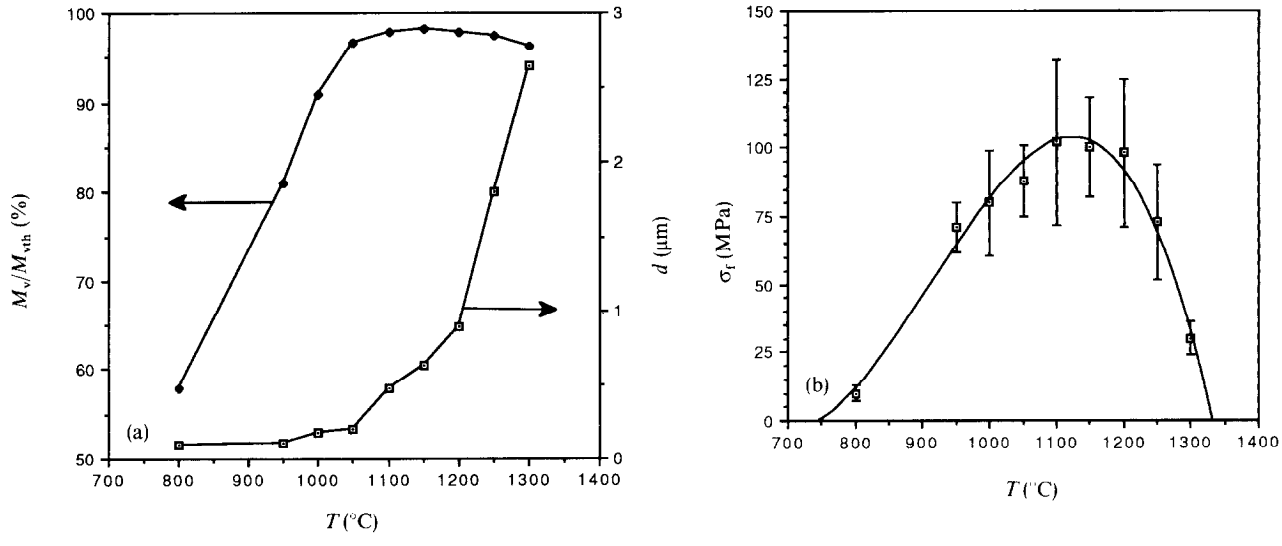

Figure 10 (a) Density and average grain size, and (b) flexural strength versus sintering temperature for pure HAP.

1000 p.p.m. magnesium delays the $\beta \rightarrow \alpha$ transformation in TCP [23]. First, as for pure HAP, the strength increases with the density; the grain size is constant up to 1150 °C. Next, when the densification is over, the strength decreases whereas the grain size increases. The strength increases again, coinciding for both samples with the appearance of α-TCP. For temperatures higher than 1400 °C the flexural strength breaks down because the samples are degraded following the decomposition of HAP into α-TCP and

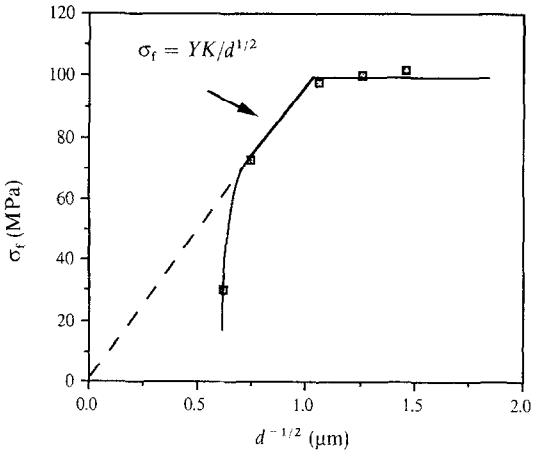

Figure 11 Relationship between the average grain size and the flexural strength of pure sintered HAP.

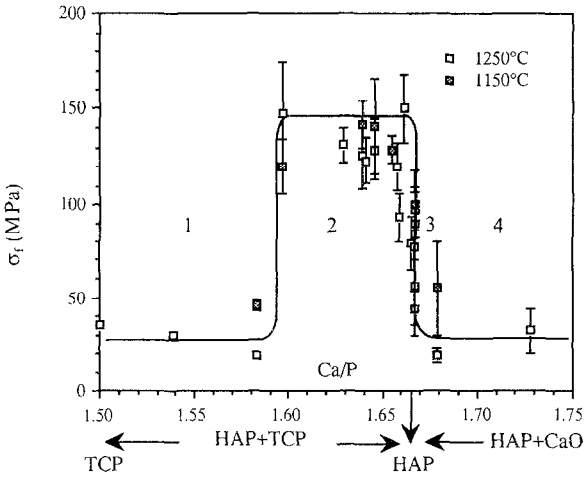

Figure 12 Influence of Ca/P on the flexural strength: (□) 1250 °C and (■) 1150 °C.

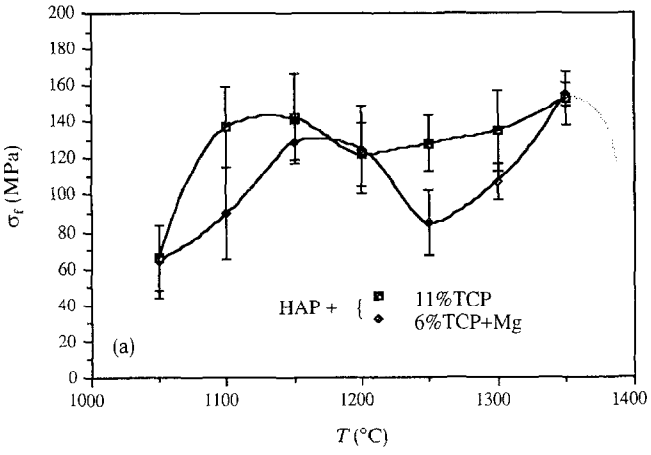

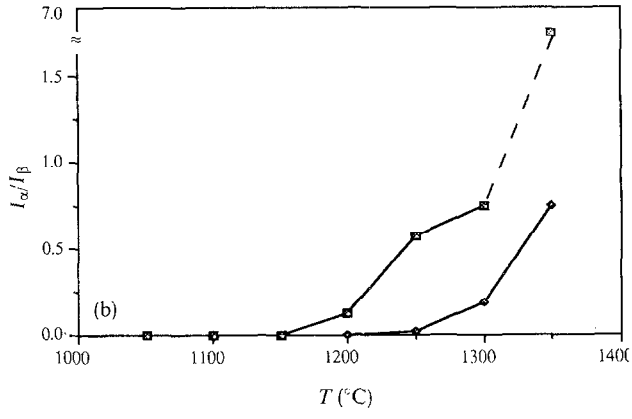

Figure 13 Evolution of (a) the flexural strength, (■) HAP + 11% TCP and (◆) HAP + 6% TCP + Mg, and (b) the TCP $\alpha \rightarrow \beta$ transformation versus the sintering temperature.

TCPM. The strengthening of HAP by α-TCP may be partially due to the surface layer of TCP. The transformation of β-TCP into α-TCP produces a volume increase which introduces compressive stress in the surface. It is assumed that the compression reduces the size of the critical flaws located near the surface, increasing the correlated failure strength [24].

4. Conclusion

The influence of the initial composition (Ca/P) of the powder on the final mechanical properties of the sintered solid has been proven. The sintering of HAP is not affected by TCP up to 40 wt %. CaO as a secondary phase in HAP lowers the flexural strength, whereas the superficial layer of α-TCP improves the mechanical behaviour of HAP. The best results are not obtained for the stoichiometry, but for the composite HAP + TCP with a Ca/P ratio ranging between 1.60 and 1.66.

References

1. A. POSNER and F. BETTS, *Acta Chem. Res.* **8** (1975) 273.
2. M. JARCHO, C. BOLEN, M. THOMAS, J. BOBICK, J. KAY and R. DOREMUS, *J. Mater. Sci.* **11** (1976) 2027.
3. M. JARCHO, J. KAY, K. GUMAER, R. DOREMUS and H. DROBECH, *J. Bioengng* **1** (1977) 79.
4. L. FEENSTER and K. DE GROOT, in "Bioceramics of calcium phosphates", edited by K. de Groot (CRC Press, Boca Raton, Florida, 1983) p. 131.
5. P. DUCHEYNE, L. HENCH, A. KAGAN, M. MARTENS, A. BURSSENS and J. MULIER, *J. Biomed. Mater. Res.* **14** (1980) 225.
6. JENN-MING WU and TUNG-SHENG YE, *J. Mater. Sci.* **23** (1988) 3771.
7. G. DE WITH and A. J. CORBIJN, *ibid.* **24** (1989) 3411.
8. C. KLEIN, A. DRIESSEN and K. DE GROOT, *Biomaterials* **5** (1984) 157.
9. P. RIBOUD, *Ann. Chim.* **8** (1973) 381.
10. A. ROYER, Thèse, INP, Grenoble (1990).
11. M. MATHEW, L. W. SCHROEDER, B. DICKENS and W. E. BROWN, *Acta Crystallogr.* **33** (1977) 1325.
12. H. FÜREDI-MILHOFER, V. HLADY, F. S. BAKER, R. A. BEEBE, N. WOLEJKO WIKHOLM and J. S. KITTELBERGER, *J. Colloid Interf. Sci.* **70** (1979) 1.
13. J. C. TROMBE, *Ann. Chim.* **8** (1973) 251.
14. J. C. HEUGHEBAERT, Thèse, INP, Toulouse (1977).
15. J. ARENDS, J. CHRISTOFERSEN, M. R. CHRISTOFERSEN, H. EEKERT, B. O. FOWLER, J. C. HEUGHEBAERT, G. H. NANCOLLAS, J. P. YESINOWSKI and S. J. ZAWACKI, *J. Cryst. Growth* **84** (1987) 515.

16. R. J. BROOK, *Treatise Mater. Sci. Technol.* **9** (1976) 331.
17. F. F. LANGE and B. J. KELLETT, *J. Amer. Ceram. Soc.* **72** (1989) 735.
18. R. W. RICE, S. W. FREIMAN, R. C. POHANKA, J. J. MECHOLSKY, JR and C. CM. WU, *Fracture Mech. Ceram.* **2** (1974) 849.
19. N. McN. ALFORD, K. KENDALL, W. J. CLEGG and J. D. BIRCHALL, *Adv. Ceram. Mater.* **3** (1988) 113.
20. G. DE WITH, H. J. A. VAN DIJK, N. HATTU and K. PRIJS, *J. Mater. Sci.* **16** (1981) 1592.
21. M. AKAO, H. AOKI and K. KATO, *ibid.* **16** (1981) 809.
22. R. W. RICE, *J. Amer. Ceram. Soc.* **52** (1969) 420.
23. B. DICKENS, L. W. SCHROEDER and W. E. BROWN *J. Solid St. Chem.* **10** (1974) 232.
24. D. J. GREEN, *J. Amer. Ceram. Soc.* **66** (1983) 807.

Received 29 April 1991
and accepted 21 January 1992